EARTHQUAKE ENGINEERING AND STRUCTURAL DYNAMICS
*Earthquake Engng. Struct. Dyn.* **28**, 1405–1425 (1999)

# FUNDAMENTAL CONSIDERATIONS FOR THE DESIGN OF NON-LINEAR VISCOUS DAMPERS

GOKHAN PEKCAN*†, JOHN B. MANDER‡ AND STUART S. CHEN‡

*Department of Civil, Structural and Environmental Engineering, State University of New York at Buffalo, Buffalo, NY 14260, U.S.A.*

## SUMMARY

Two interrelated issues related to the design of non-linear viscous dampers are considered in this paper: structural velocities and equivalent viscous damping. As the effectiveness of non-linear viscous dampers is highly dependent on operating velocities, it is important to have reliable estimates of the true velocity in the device. This should be based on the *actual* relative structural velocity and not the commonly misused spectral pseudo-velocity. This is because if spectral pseudo-velocities (PSV) are used, they are based on design displacements ($S_v = \omega_0 S_d$) and are thus fundamentally different from the *actual* relative structural velocity. This paper examines the difference between these two velocities, and based on an extensive study of historical earthquake motions proposes empirical relations that permit the designer to transform the well-known spectral pseudo-velocity to an *actual* relative structural velocity for use in design. Non-linear static analysis procedures recommended in current guidelines for the design of structural systems with supplement damping devices are based on converting rate-dependent device properties into equivalent viscous damping properties based on an equivalent energy consumption approach. Owing to the non-linear velocity dependence of supplemental devices, an alternative approach for converting energy dissipation into equivalent viscous damping is advanced in this paper that is based upon *power consumption* considerations. The concept of a *normalized damper capacity* ($\varepsilon$) is then introduced and a simple design procedure which incorporates power equivalent linear damping based on *actual* structural velocities is presented. Copyright © 1999 John Wiley & Sons, Ltd.

KEY WORDS: damping; actual velocity spectrum; non-linear damper; normalized damper capacity; power consumption; design

## INTRODUCTION

Earthquake response spectra have become the standard design tool to characterize the frequency content of a ground motion and the seismic force demand on a structural system. It is customary to generate linear elastic response spectra for various viscous damping ratios in terms of the

* Correspondence to: Gokhan Pekcan, Department of Civil, Structural and Environmental Engineering, State University of New York at Buffalo, 212 Ketter Hall, Buffalo, NY 14260, U.S.A.
† Post Doctoral Research Associate
‡ Associate Professor

*Received 10 April 1999*
CCC 0098–8847/99/111405–21$17·50 *Revised 10 June 1999*
 *Accepted 18 June 1999*

maximum value of the relative displacement. Thus for each natural period of vibration the ordinate of the spectral displacement ($S_d$) can be plotted. From this the pseudo-relative velocity $S_v$ ($= \omega_0 S_d$) and pseudo-acceleration $S_a (= \omega_0^2 S_d = \omega_0 S_v)$ can be derived for the entire range of natural circular frequencies $\omega_0 (= 2\pi/T_0$ rad/sec). This convenient and simple interrelationship is the basis for deriving design forces in structural systems, as the pseudo-acceleration is directly related to the maximum forces in the structure. Because the three quantities ($S_d$, $S_v$, $S_a$) are interrelated, they can also be conveniently expressed in a single plot in the form of the well-known tripartite response spectra.

An alternative graphical form of ground motion representation has recently come into vogue where the seismic demand spectrum is expressed as a dimensionless spectral pseudo-acceleration vs. spectral displacement plot. This is convenient form of presenting earthquake design spectra as it permits the superposition of non-linear structural capacity in the form of a normalized base shear vs. displacement (pushover curve). The composite graph is commonly referred to as the capacity-spectrum method for analysis and/or design. By estimating the effective viscous damping present in the non-linear structure, it is possible to directly estimate the response displacement. See for example Kircher[1], Freeman[2] and Mahaney *et al.*[3] The capacity-spectrum approach has also been adopted in the NEHRP Guidelines for Seismic Rehabilitation of Buildings and its Commentary[4,5] (FEMA 273/274) which provide methodologies for designing supplemental energy dissipating systems such as linear/non-linear viscous dampers.

It is common in both design and retrofit of structural building systems to approximate the real multi-degree-of-freedom (MDOF) system with an equivalent single-degree-of-freedom (SDOF) idealization such that the latter represents the most relevant characteristics of the former. In this way, any preliminary attempt to design a supplemental damping system for a structure can be simplified allowing the designer to use pre-defined response/demand spectra. However, as mentioned previously, response spectra used for the design of structures subjected to ground motions are typically based on conventional formulations of mathematical models which involve (classical viscous) linear damping. As structural engineers are most familiar with classical viscous damping it is considered essential to develop design formulations that continue to maintain notions of 'equivalent' viscous damping even though many supplemental damping devices are non-linear in nature. It must be noted that the accuracy of design and retrofit methods for building and bridge structures may largely depend on the 'quality' of the linearized parameters compared to their exact values. This is particularly important in the design of supplemental damping systems whose characteristics are primarily functions of velocity.

In fact, equivalent linear damping properties of non-linear viscous devices at given structural response amplitudes are traditionally determined based on pseudo-velocities using an energy formulation.[6] However, this study contends that it is more desirable to use the *actual* structural velocity in order to obtain consistent and more accurate estimates of damping system characteristics in terms of linearized quantities. Consequently, any attempt to predict the behaviour of such systems, in general, should be based on the *actual* velocity rather than pseudo-velocity response parameters. Unfortunately, *actual* velocity response is usually not readily available in the form of response spectra. Therefore, this paper reviews important characteristics of response spectra and then proposes a simplified period-dependent transformation between pseudo and *actual* velocities. Next, the classical energy balance method, which is customarily employed in linearization studies and adopted in FEMA 273/274,[4,5] is reviewed. A new approach based on considering power consumption equivalence between a viscously damped system and a system possessing non-linear devices is proposed and the notion of normalized damper capacity is introduced.

 

## THE DIFFERENCE BETWEEN ACTUAL AND PSEUDO-VELOCITY SPECTRA

Response spectra can be divided into various period ranges for which distinct observations can be made. The characteristics of each of these regions become very important when deriving design response spectra. In general, it can be observed that in the short period (high-frequency) range (which implies a stiff structure), pseudo-acceleration approaches the peak ground acceleration (PGA) as the system deforms very little and the mass moves with the ground. This observation is valid for all damping values. Similarly, in the long period (low-frequency) range (flexible structures), the maximum displacement response is practically equal to the maximum ground displacement whereas in the intermediate period range the displacement response is somewhat amplified beyond the ground displacement. However, in this intermediate period range, there is a near constant amplification factor for pseudo-acceleration response for a given viscous damping ratio. This amplification factor becomes smaller for higher damping ratios. A nearly constant velocity response is observed in the intermediate period range.

The maximum relative displacement response, $S_d$ of a SDOF system subjected to a ground acceleration $p(t)$ may be expressed by the well-known *Duhamel* integral as:[7]

$$S_d = \left| \frac{1}{\omega_0} \int_0^t p(\tau) \sin \omega_d (t-\tau) \exp(-\xi\omega_0(t-\tau))\, d\tau \right|_{max} \tag{1}$$

when small critical viscous damping is assumed ($\omega_d = \omega_0\sqrt{1-\xi^2} \cong \omega_0$). The displacement response can be differentiated with respect to time to obtain the corresponding *actual* relative velocity response from which the maximum response can be calculated as

$$V = \left| \int_0^t p(\tau) \cos \omega_0 (t-\tau)\, d\tau \right|_{max} \tag{2}$$

It must be noted that viscous damping ratio $\xi$, is assumed to be zero in the above expression for simplicity. Moreover, using equation (1) with $\xi = 0$, the relative pseudo-velocity can be written as

$$S_v = \left| \int_0^t p(\tau) \sin \omega_0 (t-\tau)\, d\tau \right|_{max} \tag{3}$$

It is clear from equations (2) and (3) that the *actual* structural velocity ($V$) and pseudo-velocity ($S_v$) are *different* even for zero damping, since the former involves a *cosine* term whereas the latter expression has a *sine* term. It can be shown that the difference between the two response values becomes more pronounced for long period systems as well as for high damping ratios. In general, pseudo-relative velocity spectra ($S_v$) values are consistently higher than the *actual*-relative spectra ($V$) in the low period range, and become nearly the same in the medium period range for low damping values. The lower and upper period limits of this region depend on the frequency content of the velocity trace of the ground motion. In other words, the broader the band of frequencies present in the ground motion, the broader is the range of natural periods over which the pseudo and *actual* velocities are similar. Furthermore, pseudo-relative velocity ($S_v$) is unconservative in the high period region as the *actual*-relative velocity ($V$) approaches the maximum ground velocity ($v_g$) while pseudo-velocity approaches zero as $T_0 \to \infty$.

Following a similar discussion, it can be shown that the pseudo-acceleration is the same as the maximum *actual* acceleration when there is no damping in the system. However, for higher damping values, pseudo-acceleration starts to diverge from the maximum acceleration. The

 

pseudo-acceleration is typically less than the maximum *actual* acceleration. Constantinou *et al.*[8] have suggested an approximate relationship between the maximum and pseudo-acceleration by assuming that during the cycle of maximum response, the analysed SDOF system conforms to harmonic motion with frequency $\omega_0$:

$$A = (f_1 + 2\xi f_2) S_a \tag{4}$$

in which $f_1 = \cos[\tan^{-1}(2\xi)]$ and $f_2 = \sin[\tan^{-1}(2\xi)]$.

The difference between maximum and pseudo-acceleration, however, has less significance than the difference between the corresponding velocities from a design standpoint. The main reason for this is that the current seismic design codes specify the earthquake excitation in the form of acceleration response spectra with amplification factors that indirectly consider the aforementioned pitfall. In case of a classically damped system, the difference between pseudo and *actual* velocities can still be considered insignificant. However, if non-linear viscous devices are present in the system, the high levels of damping associated with these devices is heavily dependent on the velocities. Therefore, the difference between pseudo and *actual* velocity becomes quite significant.

In previous applications of spectral analysis and design approaches[6] to non-classically damped systems, the spectral values of relative velocity were approximated by the corresponding pseudo-velocity values. While it may lead to results of reasonable accuracy under certain conditions, this approximation is clearly not generally valid. Hence, there is a need to re-examine the issues involved in the application of classical analysis and design methods to non-classically damped systems such as those with non-linear rate-dependent devices. Note that the resisting force provided by a non-linear rate-dependent damping device is given by $F_D = \mathrm{sgn}(\dot{x}) c_\alpha |\dot{x}|^\alpha$ where $\alpha < 1{\cdot}0$.

## RELATIONSHIP BETWEEN ACTUAL AND PSEUDO-RELATIVE VELOCITY SPECTRA

Based on the above observations, a general empirical relationship between pseudo and *actual* maximum velocity is derived herein using a set of 36 earthquake ground motions. In order to facilitate direct comparison of results, each record was scaled such that the maximum ground velocity was $v_{g\max} = 1$ m|sec. The ground motions used are listed in Table I. Mean pseudo and *actual* relative velocity spectra for these ground motions are plotted in log–log scale velocity-period graphs in Figure 1 for $T_0 = 0$–10 sec and viscous damping ratios, $\xi$ of 5, 10, 20, 30, 40 and 50 per cent.

The following set of relationships are proposed for three different period ranges mentioned above

$$V = S_v \begin{cases} \left(\dfrac{T_0}{T_1}\right)^{\alpha_1} \left(\dfrac{T_0}{T_m}\right)^{\alpha_m}, & 0 < T_0 < T_1 \\ \left(\dfrac{T_0}{T_m}\right)^{\alpha_m}, & T_1 \leqslant T_0 \leqslant T_u \\ \left(\dfrac{T_0}{T_m}\right)^{\alpha_m} \left(\dfrac{T_0}{T_u}\right)^{\alpha_u}, & T_0 > T_u \end{cases} \tag{5}$$

 

Table I. Earthquake ground motions

| Ground motion | Station | Direction | PGA, g | PGV, m/s | PGD, m |
|---|---|---|---|---|---|
| Tabas, Sep 78 | Tabas/Iran | N/A | 0·812 | 0·856 | 0·430 |
| Loma Prieta, 89 | Los Gatos P.C. | N/A | 0·717 | 1·728 | 0·646 |
| Loma Prieta, 89 | Lex. Dam | N/A | 0·686 | 1·787 | 0·566 |
| C. Mendocino, 92 | Petrolia | N/A | 0·655 | 0·929 | 0·414 |
| Erzincan, 92 | Erzincan/Turkey | N/A | 0·432 | 1·192 | 0·421 |
| Landers, 92 | Lucerne | N/A | 0·713 | 1·359 | 1·566 |
| Northridge, 94 | Rinaldi R.St. | N/A | 0·889 | 1·746 | 0·383 |
| Northridge, 94 | Sylmar, Olive | N/A | 0·732 | 1·219 | 0·305 |
| Kobe, 95 | Kobe, JMA | N/A | 1·088 | 1·698 | 0·402 |
| Kobe, 95 | Takatori | N/A | 0·786 | 1·738 | 0·560 |
| Imperial Valley, 79 | Array 5 | N230 | 0·374 | 0·880 | 0·541 |
| Imperial Valley, 79 | Array 5 | N140 | 0·527 | 0·438 | 0·246 |
| Imperial Valley, 79 | Array 6 | N140 | 0·376 | 0·627 | 0·275 |
| Imperial Valley, 79 | Array 6 | N230 | 0·436 | 1·061 | 0·578 |
| Imperial Valley, 79 | Array 7 | N140 | 0·333 | 0·447 | 0·208 |
| Imperial Valley, 79 | Array 7 | N230 | 0·462 | 1·063 | 0·418 |
| Imperial Valley, 79 | Bounds Corner | N140 | 0·587 | 0·437 | 0·131 |
| Imperial Valley, 79 | Bounds Corner | N230 | 0·785 | 0·485 | 0·151 |
| San Fernando, 71 | Pacoima Dam | S16E | 1·170 | 1·156 | 0·561 |
| San Fernando, 71 | Pacoima Dam | S74W | 1·070 | 0·590 | 0·156 |
| Northridge, 94 | Sylmar CH. | 360° | 0·843 | 1·291 | 0·313 |
| Northridge, 94 | Sylmar CH. | 90° | 0·604 | 0·776 | 0·188 |
| Northridge, 94 | Santa Monica | 360° | 0·369 | 0·250 | 0·074 |
| Northridge, 94 | Santa Monica | 90° | 0·883 | 0·411 | 0·129 |
| Northridge, 94 | Tarzana | 360° | 0·989 | 0·778 | 0·334 |
| Northridge, 94 | Tarzana | 90° | 1·778 | 1·064 | 0·289 |
| Northridge, 94 | Newhall F.S. | 360° | 0·589 | 0·952 | 0·393 |
| Northridge, 94 | Newhall F.S. | 90° | 0·583 | 0·741 | 0·187 |
| Northridge, 94 | Arleta F.S. | 360° | 0·308 | 0·231 | 0·112 |
| Northridge, 94 | Arleta F.S. | 90° | 0·344 | 0·396 | 0·162 |
| Kobe, 95 | Kobe, KOB/Japan | NS | 0·833 | 0·918 | 0·214 |
| Kobe, 95 | Kobe, KOB/Japan | EW | 0·629 | 0·757 | 0·238 |
| Imperial Valley, 40 | El Centro | S00E | 0·348 | 0·396 | 0·169 |
| Imperial Valley, 40 | El Centro | S90W | 0·214 | 0·489 | 0·150 |
| Kern County, 52 | Taft L. Tunnel | N21E | 0·156 | 0·181 | 0·080 |
| Kern County, 52 | Taft L. Tunnel | S69E | 0·179 | 0·175 | 0·100 |
| Average | — | — | 0·629 | 0·844 | 0·327 |

A non-linear least-squares regression analysis was used to establish the parameters in equation (5), i.e. period ranges and corresponding powers. Results of this analysis are presented in Table II along with the respective correlation coefficients, $r^2$. It is evident that good agreement is obtained throughout the entire range of periods from $T_0 = 0{\cdot}01$–10 sec.

## TRANSFORMATION FROM PSEUDO TO ACTUAL RELATIVE VELOCITY FOR DESIGN PURPOSES

For design purposes, ground motions are expressed in terms of spectral accelerations. Therefore, the ground motions listed in Table I were scaled to a PGA = 0·6g and linear response

 

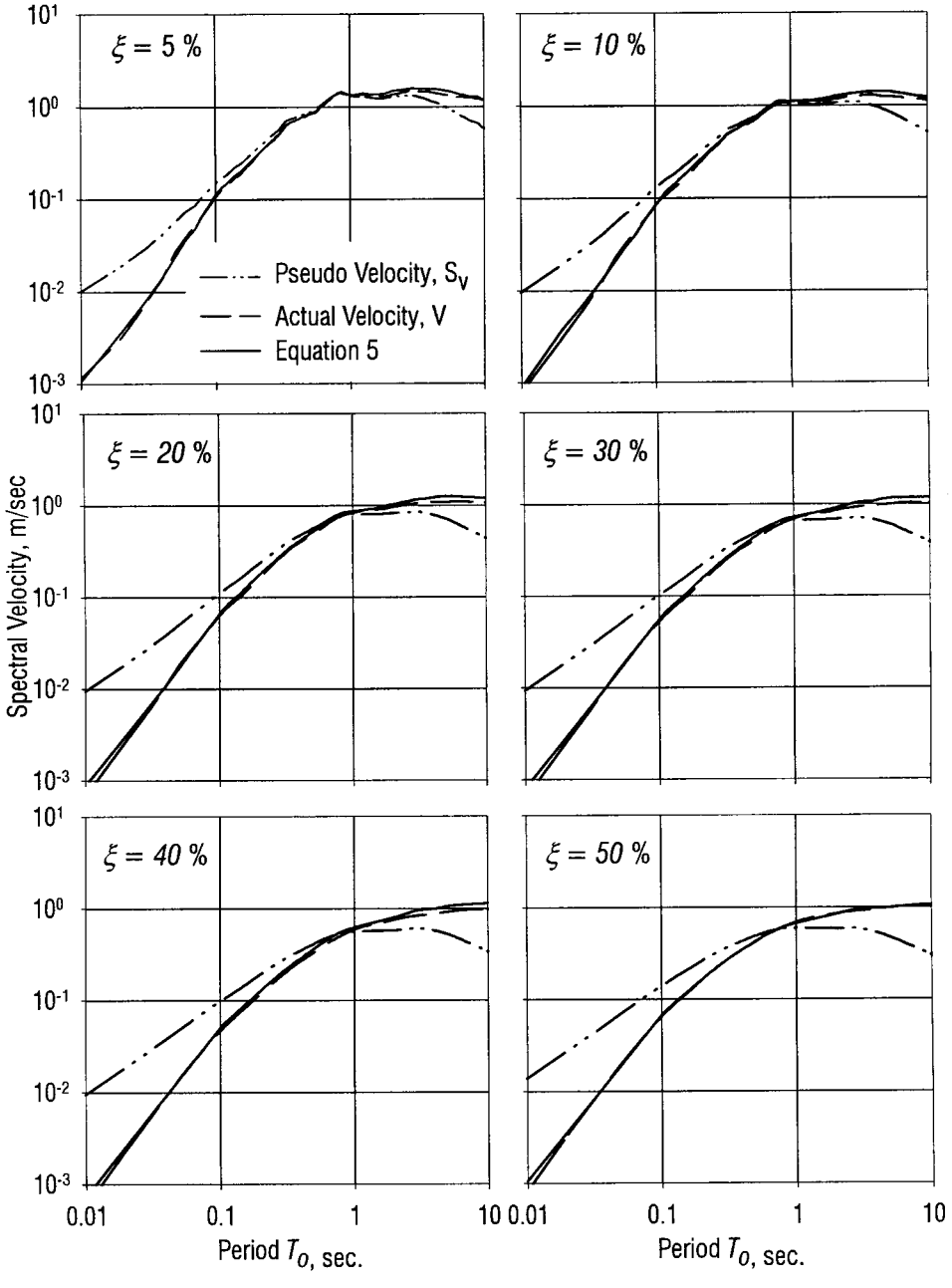


Figure 1. Mean pseudo-actual velocity spectra transformation

 

Table II. Regression results

| Parameter definition | Equation | $r^2$ |
|---|---|---|
| Upper limit period, $T_u$ | $T_u = 3{\cdot}149\xi + 3{\cdot}112$ | 0·98 |
| Intermediate limit period, $T_m$ | $T_m = 0{\cdot}064\xi + 0{\cdot}756$ | 0·96 |
| Lower limit period, $T_l$ | $T_l = 0{\cdot}042\xi + 0{\cdot}113$ | 0·96 |
| Exponent, $\alpha_u$ | $\alpha_u = 0{\cdot}607\xi + 0{\cdot}489$ | 0·99 |
| Exponent, $\alpha_m$ | $\alpha_m = 0{\cdot}455\xi + 0{\cdot}132$ | 0·98 |
| Exponent, $\alpha_l$ | $\alpha_l = 0{\cdot}450\xi + 0{\cdot}729$ | 0·99 |

spectra were generated for viscous damping ratios of $\xi = 5$, 10, 20, 30 and 40 per cent. A period range of $T_0 = 0$–3 sec was chosen, since it covers the natural periods that are most relevant to most building structures. Pseudo-relative velocity ($S_v = T_0 S_a/2\pi$) spectra are plotted in Figure 2 together with corresponding *actual* velocities. The difference between *actual* and pseudo-velocities, as described above, can also be seen in these figures. The following transformation is proposed for 5 per cent equivalent viscous damping based on the general expression given in equation (5) and for the period range considered

$$V^{5\%} = S_v^{5\%} \left(\frac{T_0}{0{\cdot}75}\right)^{0{\cdot}15} \quad 0 \leqslant T_0 \leqslant 3 \text{ sec} \tag{6}$$

Actual velocity spectra for higher damping ratios can be determined in an approximate sense using the well-known demand reduction factors $B_s$ and $B_l$ for the short- and long-period ranges, respectively. A regression analysis was performed on the values recommended by Newmark and Hall[9] to obtain an empirical expression. The following relationships are proposed with the results plotted and compared with the Newmark–Hall values in Figure 3:

$$B_s = \left(\frac{\xi}{0{\cdot}05}\right)^{0{\cdot}5} \quad \text{and} \quad B_l = \left(\frac{\xi}{0{\cdot}05}\right)^{0{\cdot}3} \tag{7}$$

In sum, the *actual* velocity spectra for higher damping ($V_\xi$) can be obtained using equations (6) and (7) as follows:

$$V_\xi = \left(\frac{T_0}{0{\cdot}75}\right)^{0{\cdot}15} \begin{cases} \dfrac{S_v^{5\%}}{B_s} & 0 \leqslant T_0 \leqslant T_{sl} = \dfrac{C_v}{2{\cdot}5C_a} \\ \dfrac{S_v^{5\%}}{B_l} & 0{\cdot}75\,\dfrac{B_s}{B_l} \leqslant T_0 \leqslant 3 \text{ sec.} \end{cases} \tag{8}$$

where $C_v$ is the effective peak ground velocity, $C_a$ the effective peak ground acceleration, and $T_{sl}$ the period that marks the transition between short- and long-period ranges.

It should be noted that equation (8) is not valid for the period range $T_{sl} = C_v/2{\cdot}5C_a < T_0 < 0{\cdot}75(B_s/B_l)$; instead, a linear relationship is assumed for this intermediate region.

As mentioned above, in present practice response spectra approaches using appropriate equivalent linear properties are nowadays used in the design of structures. This approach could be easily implemented in a design procedure that involves supplemental damping systems, particularly if the relevant non-linear properties of such systems can be reliably linearized.

 

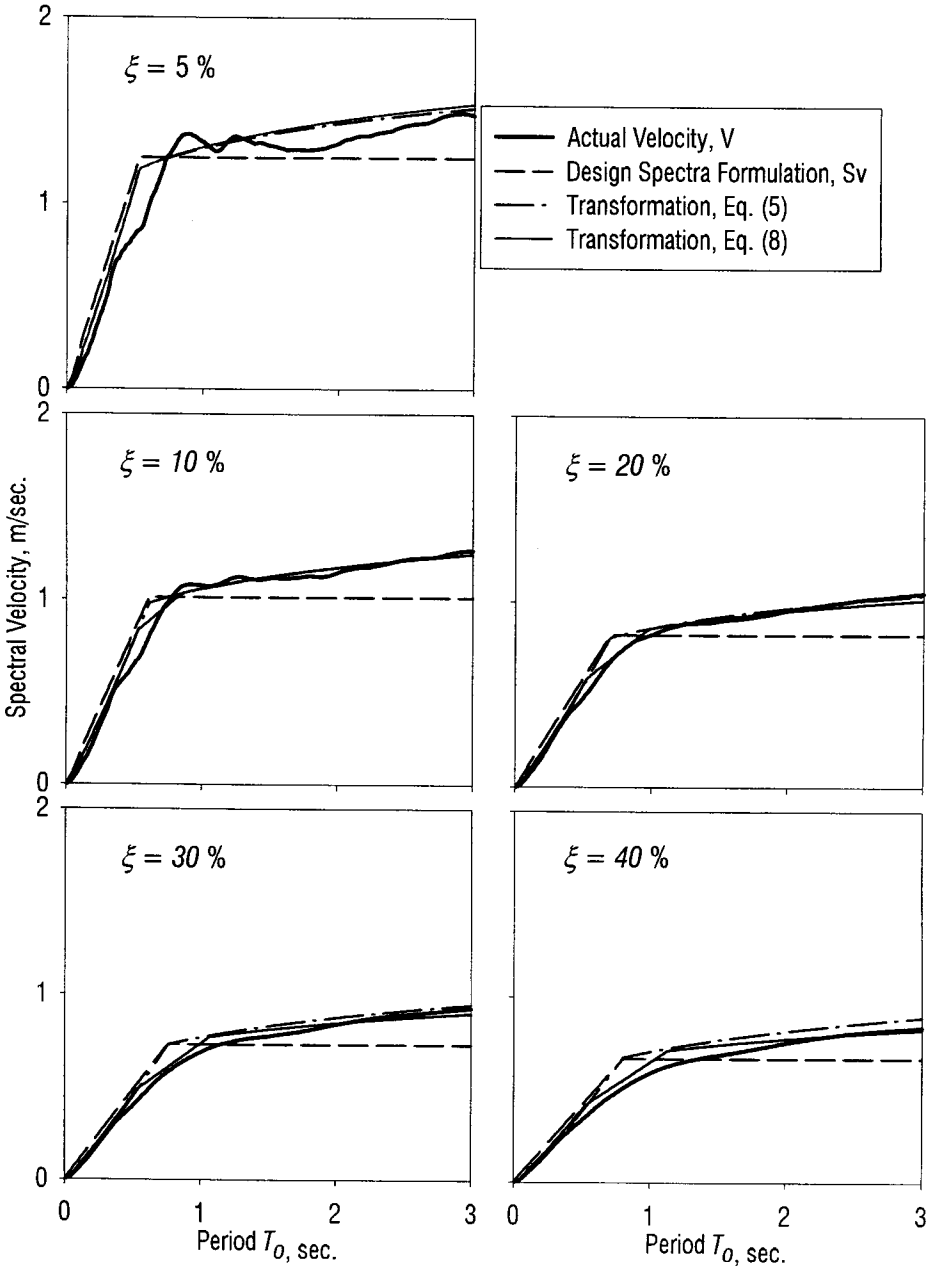


Figure 2. Design spectra formulation of pseudo-actual velocity transformations

 

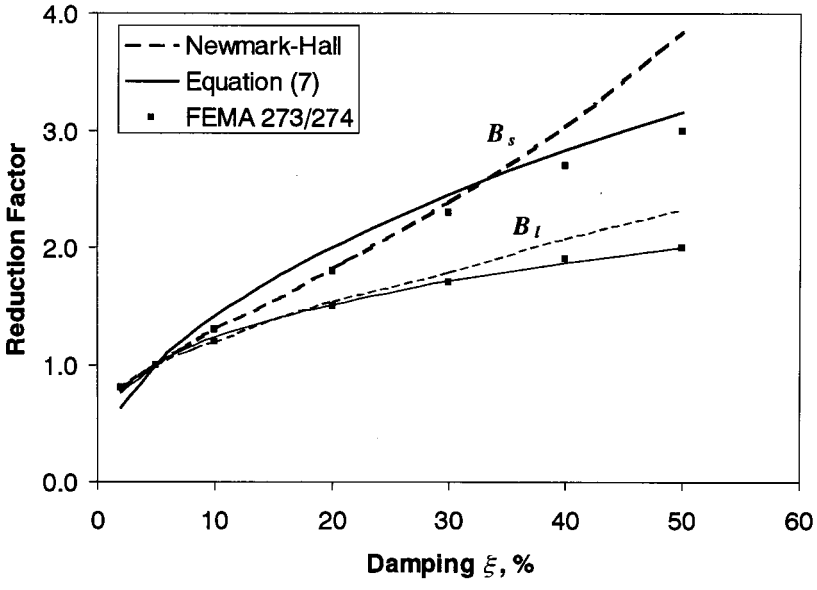


Figure 3. Long- and short-period demand reduction factors

Therefore, a simple linearization technique is described for non-linear [viscous] damping systems in what follows.

## LINEARIZATION OF NON-LINEAR ($\alpha \neq 1$) VISCOUS DAMPING

One of the most common methods for defining equivalent viscous damping is to equate the energy dissipated in a vibration cycle of the actual non-linear system to that of equivalent viscous system. Applying the energy balance method to non-linear viscous damping devices which can be modelled using the following equation:

$$F_{\mathrm{D}} = \mathrm{sgn}(\dot{x}_{\mathrm{D}}) c_{\alpha} |\dot{x}_{\mathrm{D}}|^{\alpha} \tag{9}$$

where $\dot{x}_{\mathrm{D}}$ is the damper velocity, $c_{\alpha}$ the damper coefficient, and $F_{\mathrm{D}}$ the damper force.

Constantinou[6] has shown that the work done (dissipated energy) in one cycle of sinusoidal loading can be written as

$$W_{\mathrm{d}} = \int_0^{T_0} F_{\mathrm{D}} \dot{x}_{\mathrm{D}} \, \mathrm{d}t \tag{10}$$

where $T_0 = 2\pi/\omega_0$ and $\dot{x}_{\mathrm{D}} = x_0 \sin \omega_0 t$.

Equation (10) can be integrated to give

$$W_{\mathrm{d}} = 2^{\alpha+2} \frac{\Gamma^2(1 + \alpha/2)}{\Gamma(2 + \alpha)} c_{\alpha} x_0^{1+\alpha} \omega_0^{\alpha} \tag{11}$$

where $\Gamma(\,)$ is the gamma function.

 

The equivalent (added) damping[10] is calculated by equating equation (11) and the energy dissipated in equivalent viscous damping:

$$4\pi\xi_{\mathrm{d}}\omega_0 E_{\mathrm{S}} = W_{\mathrm{d}} \tag{12}$$

in which strain energy $E_{\mathrm{S}} = kx_0^2/2$. Solving equation (12) for equivalent damping ratio:

$$\xi_{\mathrm{d}} = \frac{2^{1+\alpha} c_\alpha x_0^{\alpha-1} \omega_0^{\alpha-2}}{\pi M} \frac{\Gamma^2(1+\alpha/2)}{\Gamma(2+\alpha)} \tag{13}$$

where $M$ is the mass of the system, and $x_0$ the amplitude of harmonic motion at the undamped natural frequency $\omega_0$.

Note that due to the viscous nature of this type of device, it is conveniently assumed that they possess only equivalent viscous damping characteristics.

## PROPOSED EQUIVALENT POWER CONSUMPTION APPROACH

In this study, it is contended that for velocity-dependent systems such as viscous dampers, consideration of the *rate* of energy dissipation—that is power (rather than energy)—becomes more important in seeking the equivalent linear properties for these systems. A simple method for making the transformation from the non-linear damper behaviour to equivalent viscous damping is described in what follows.

Power, by definition, is the *rate* of energy dissipation. The time-average power consumption over one cycle of sinusoidal loading can be approximated as the area under the force–velocity response curve, as shown in Figure 4 and given as

$$\bar{P} \approx \frac{F_{\mathrm{D}0}\dot{x}_{\mathrm{D}0} + F_{\mathrm{D}n}\dot{x}_{\mathrm{D}n}}{2} \approx \frac{1}{2}\sum_{i=1}^{T_0/\Delta t} (F_{\mathrm{D}_{i+1}} + F_{\mathrm{D}_i})(\dot{x}_{\mathrm{D}_{i+1}} - \dot{x}_{\mathrm{D}_i}) = \int_0^{T_0} F_{\mathrm{D}}\,\mathrm{d}\dot{x}_{\mathrm{D}} \tag{14}$$

where $\bar{P}$ is the average power consumption over one cycle of sinusoidal response, $F_{\mathrm{D}0}$, $F_{\mathrm{D}n}$ are the damper force at the beginning and at the end of the time history, respectively, $\dot{x}_{\mathrm{D}0}$, $\dot{x}_{\mathrm{D}n}$ the corresponding damper velocities, $F_{\mathrm{D}_i}$ the damper force, and $\dot{x}_{\mathrm{D}_i}$ the damper velocity.

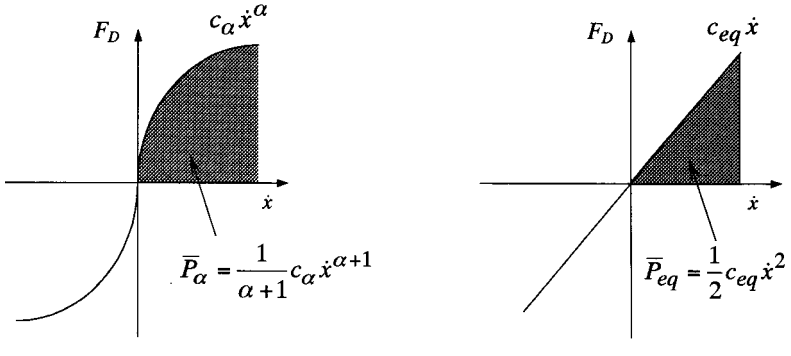


Figure 4. Equivalent power formulation

 

Thus, average power consumption over one cycle of oscillation (area under the force–velocity curve) for the non-linear damper ($c_\alpha$) is equated to that for the equivalent linear damper ($c_{eq}$) with $\alpha = 1$:

$$\bar{P}_\alpha = \bar{P}_{eq}, \quad \frac{1}{1+\alpha} c_\alpha \dot{x}_0^{\alpha+1} = \frac{1}{2} c_{eq} \dot{x}_0^2 \tag{15}$$

Solving the above equation (15) for $c_{eq}$ gives

$$c_{eq} = \frac{2}{1+\alpha} c_\alpha \dot{x}_0^{\alpha-1} \tag{16}$$

Given the customary definition of damping ratio ($\xi$) obtained from $c = 2\xi\omega_0 M$, equation (16) can be expressed as follows:

$$\xi_d = \frac{1}{1+\alpha} \frac{c_\alpha x_0^{\alpha-1} \omega_0^{\alpha-2}}{M} \tag{17}$$

## COMPARISON OF THE PROPOSED POWER AND ENERGY BASED METHODS

For comparative purposes, the respective energy and power-based formulations, equations (13) and (17), can be now written in a common format as follows:

$$\xi_d = \kappa \left( \frac{c_\alpha x_0^{\alpha-1} \omega_0^{\alpha-2}}{M} \right) \tag{18}$$

where

$\kappa = \kappa_{EN} = \dfrac{2^{1+\alpha}}{\pi} \dfrac{\Gamma^2(1+\alpha/2)}{\Gamma(2+\alpha)}$ for the energy approach and

$\kappa = \kappa_{PO} = \dfrac{1}{1+\alpha}$ for the power approach.

These coefficients are plotted for various $\alpha$ values and are compared in Figure 5. As can be seen from that figure, the power equivalent approach predicts higher damping values (17 per cent more for $\alpha = 0{\cdot}5$ and values 28 per cent more for $\alpha = 0{\cdot}2$) in general as the two curves converge to 0·5 for $\alpha = 1$. One must be cautious using any of the above formulations for small $\alpha$ powers ($\alpha < 0{\cdot}1$), since the mechanism of the devices changes from viscous (velocity dependent) to Coulomb friction type (when $\alpha \to 0$).

The equation of motion of a linear SDOF system with various non-linear viscous dampers was numerically solved to generate response spectra. Elastic response spectra are generated for 1940 Imperial Valley-El Centro N-S, 1994, Northridge-Sylmar County Hospital. Peak ground accelerations of these ground motions are scaled to 1·0 g in order to facilitate direct comparison of the results. The inherent viscous damping of the parent structure is assumed to be a standard value of $\xi_0 = 5$ per cent. The non-dimensional damper capacity $\varepsilon$ is defined as

$$\varepsilon = \frac{c_\alpha \dot{x}_{ref}^\alpha}{W} \tag{19}$$

 

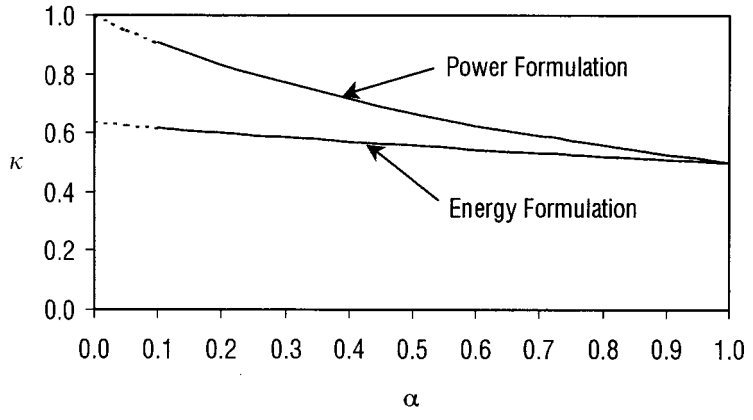


Figure 5. Comparison of equivalent damping formulations

where $W$ is the total weight of the system, and $\dot{x}_{\text{ref}} = 1$ m/sec which is a standard testing velocity for viscous dampers (Note: for some manufacturers standard testing velocity is 2 m/sec).

Introducing the non-dimensional damper capacity $\varepsilon$ into equations (13) and (17) and rearranging gives normalized damper capacities, respectively, based on energy and power equivalent formulations, as follows:

$$\varepsilon_{\text{EN}} = \xi_{\text{d}} \left( \frac{\pi}{2^{1+\alpha} g} \frac{\Gamma(2+\alpha)}{\Gamma^2(1+\alpha/2)} \dot{x}_{\xi_{\text{eff}}}^{1-\alpha} \omega_0 \right) \tag{20}$$

$$\varepsilon_{\text{PO}} = \xi_{\text{d}} \left( \frac{1+\alpha}{g} \dot{x}_{\xi_{\text{eff}}}^{1-\alpha} \omega_0 \right) \tag{21}$$

where $\dot{x}_{\xi_{\text{eff}}}$ is the *actual* velocity response of a system with total effective damping $\xi_{\text{eff}}$ (due to all possible mechanisms in the system) and $\omega_0$ the natural frequency of vibration.

Damper capacity $\varepsilon$ is calculated for equivalent (added) damping values $\xi_{\text{d}} = 5$, 15 and 35 per cent. Since the inherent viscous damping $\xi_0$ of the SDOF system is assumed to be 5 per cent, pseudo- (as well as actual) velocity values that correspond to 10, 20 and 40 per cent total viscous damping $\xi_{\text{eff}}$ are used to calculate the corresponding damper capacities given in equations (20) and (21). The equation of motion including the non-linear viscous dampers with $\alpha = 0{\cdot}5$ and $0{\cdot}2$ is solved numerically to obtain the exact response. Comparisons are given in Figures 6–9 for the two ground motions listed above. On the left-hand column, pseudo-spectral velocity response is compared for the natural period of vibrations, $T_0$ up to 10 sec as the damper capacities ($\varepsilon$) were determined from equations (20) and (21) for energy and power equivalent cases, respectively. The right-hand column of plots presents results of three different cases compared to corresponding equivalent viscous solution. These plots include results for damper capacities based on (a) *actual* velocity response ($V$), (b) pseudo-velocity response ($S_{\text{v}}$), (c) the transformation from pseudo to *actual* velocity of the equivalent linear system ($S_{\text{v}} \rightarrow V$).

As can be seen from these plots, the power equivalent approach gives either better or comparable predictions compared to the energy approach. Analysis results based on the velocity transformation generally give better predictions compared to the predictions based on the

 

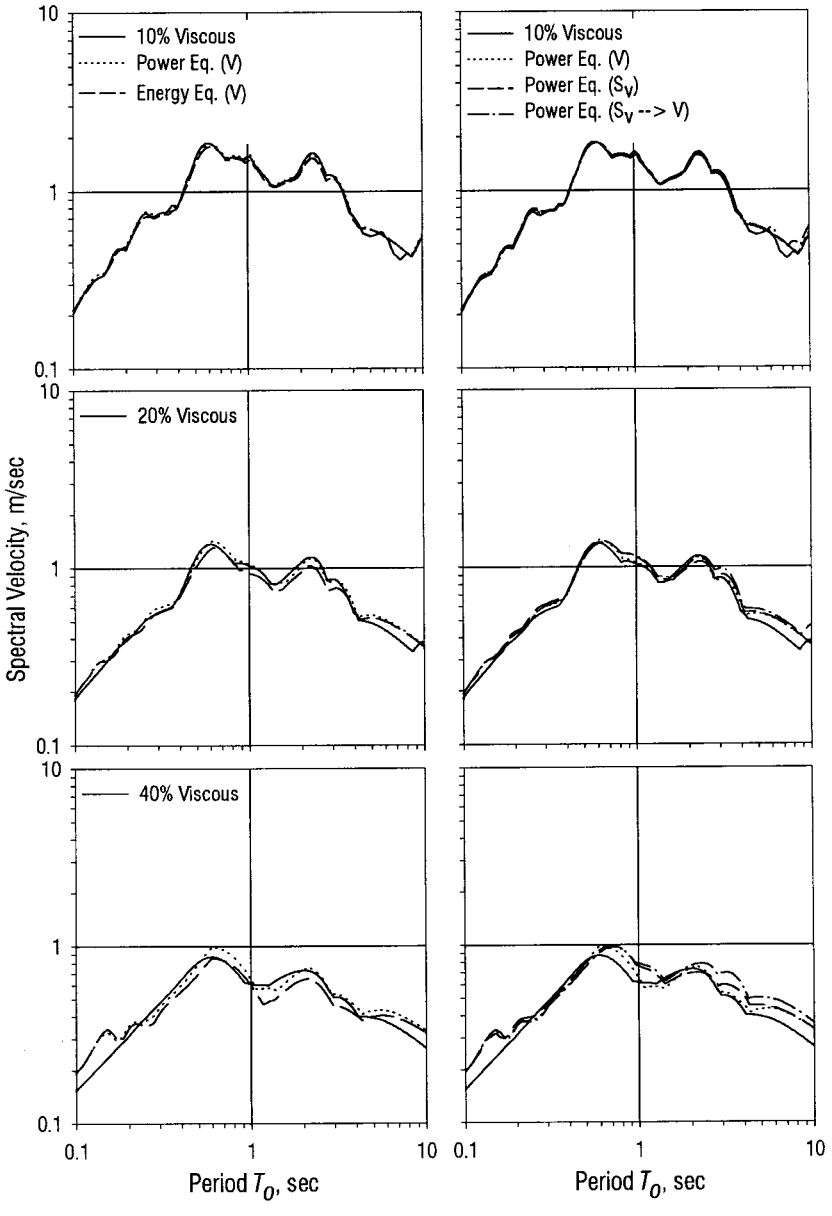


Figure 6. Comparison of energy and power approach—El Centro, $\alpha = 0{\cdot}5$

pseudo-spectral velocity. When the dynamic response is governed by ground displacements, as in the case for long period system when $T_0 > 4$ sec, the approximations in many of the cases are unconservative. However, the approximate power-based formulation gives satisfactory predictions within the range ($0 \leqslant T_0 \leqslant 4$ sec), this is the range of interest for most building and bridge structures.

 

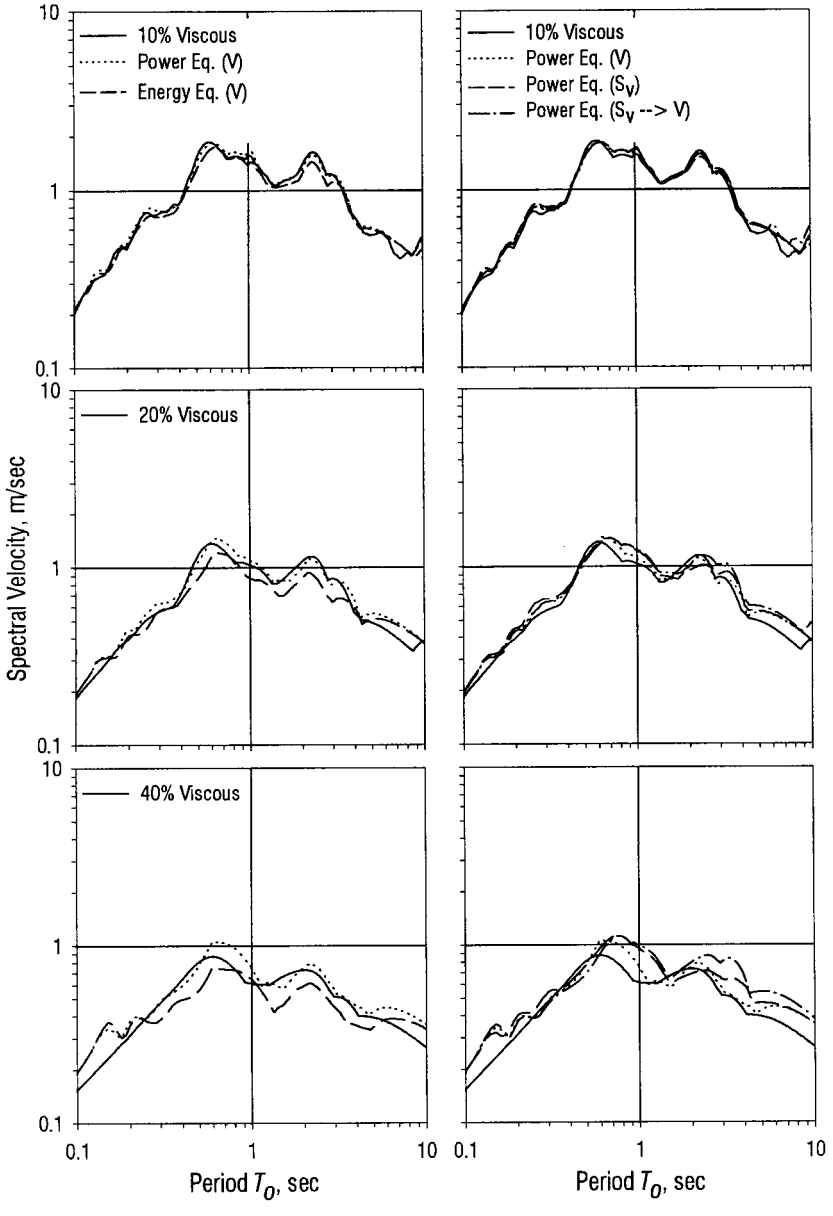


Figure 7. Comparison of energy and power approach—El Centro, $\alpha = 0{\cdot}2$

## ADDED DAMPING IN TERMS OF NORMALIZED DAMPER CAPACITY

The normalized damper capacity, $\varepsilon$ previously defined in equation (19) and the proposed velocity transformation equation (8) allow one to express the added damping due to both linear ($\alpha = 1{\cdot}0$)

 

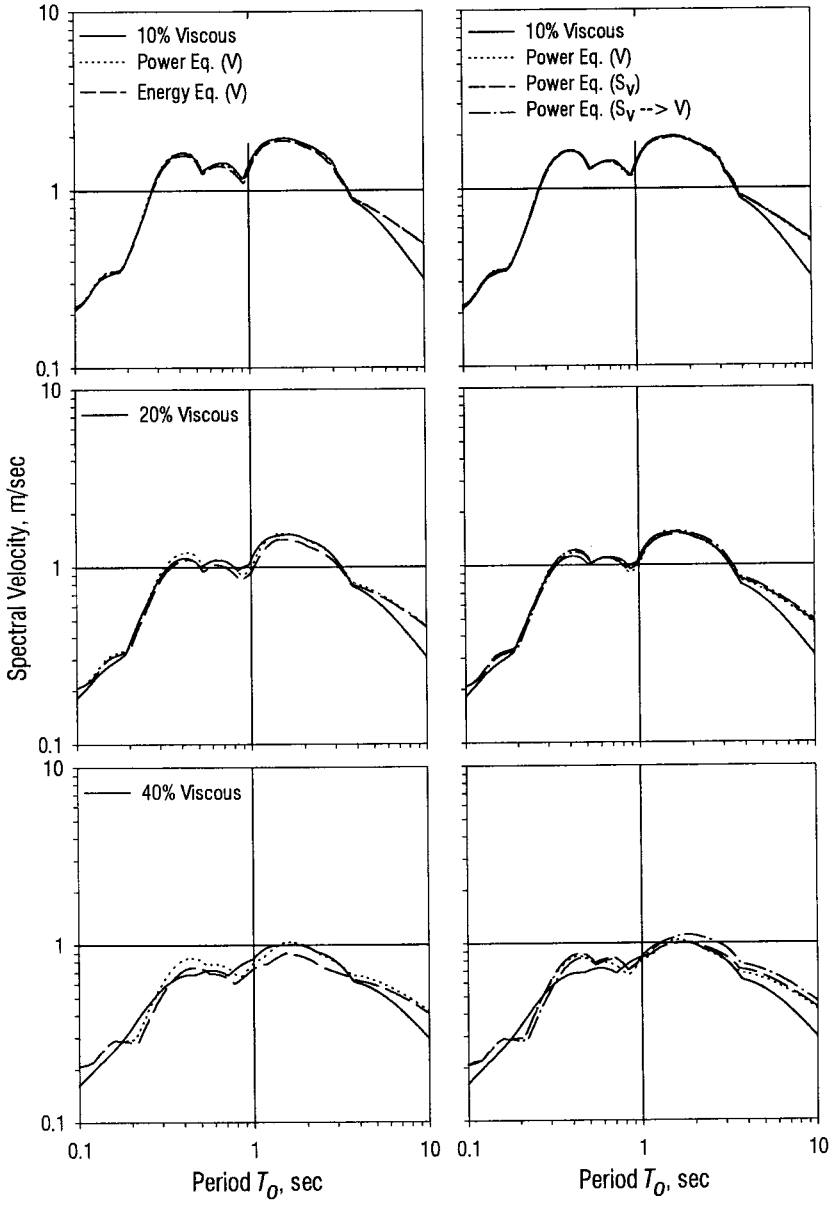


Figure 8. Comparison of energy and power approach—Sylmar C.H., $\alpha = 0{\cdot}5$

and non-linear ($\alpha < 1{\cdot}0$) viscous dampers in terms of spectral quantities—that is spectral displacement, $S_d$ and demand, $C_d$:

$$C_d = \frac{V_b}{W} \tag{22}$$

where $V_b$ is the base shear, and $W$ the seismic weight.

 

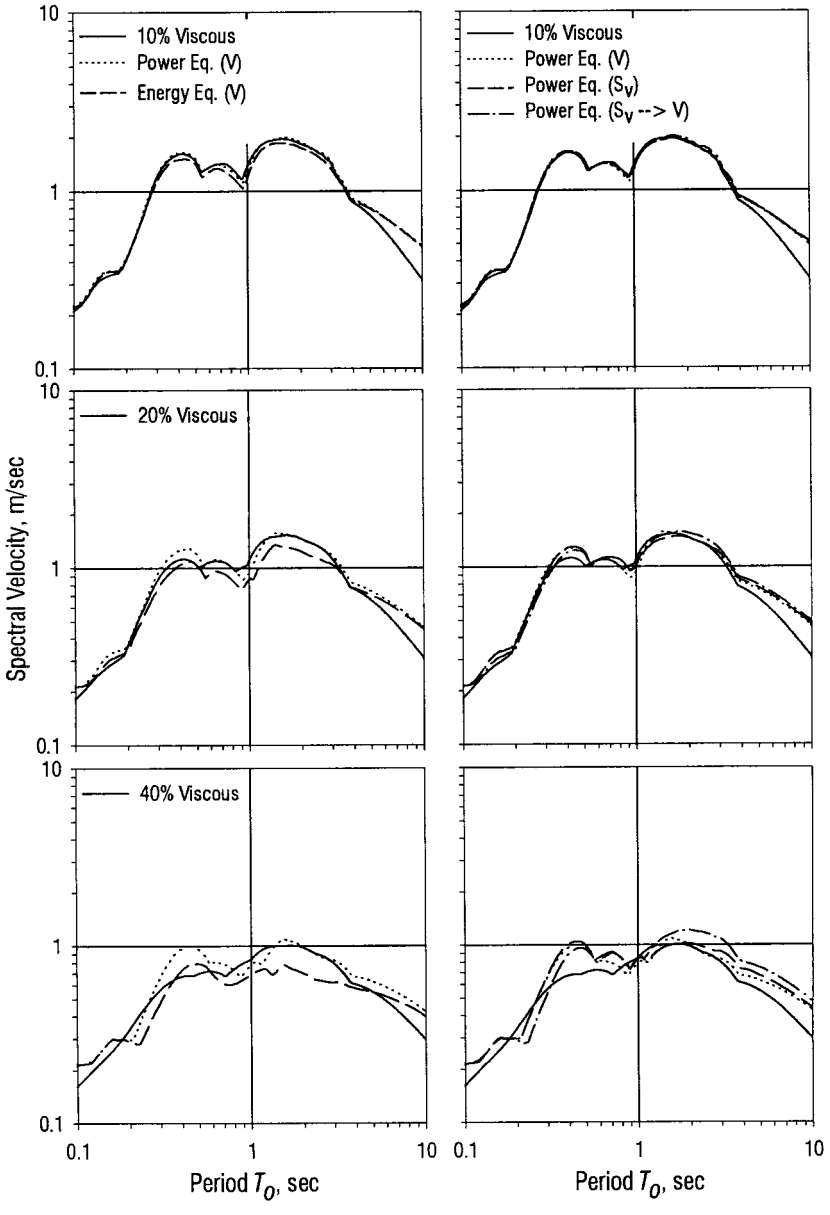


Figure 9. Comparison of energy and power approach—Sylmar C.H., $\alpha = 0{\cdot}2$

Hence, equation (8) can be used to determine the *actual* velocity in equation (21), which in turn is solved for the equivalent (added) damping to give

$$\xi_d = \frac{\varepsilon}{1+\alpha}\left(\frac{2\pi}{0{\cdot}75}\right)^{0{\cdot}15(\alpha-1)} g^{0{\cdot}5(0{\cdot}85\alpha+0{\cdot}15)} S_d^{0{\cdot}5(1{\cdot}15\alpha-0{\cdot}15)} C_d^{0{\cdot}5(0{\cdot}85\alpha-1{\cdot}85)} \tag{23}$$

where $\xi_d$ is the added damping and $\alpha$ the damper power.

 

Note that for a linear viscous damper ($\alpha = 1{\cdot}0$ and $g = 9{\cdot}81\ \mathrm{m/s^2}$), equation (23) takes the simple form

$$\xi_{d_{\alpha=1}} = 13\varepsilon\sqrt{\frac{S_d}{C_d}} \tag{24a}$$

Certain manufacturers use dampers with a silicon putty fluid[11] giving $\alpha = 0{\cdot}2$:

$$\xi_{d_{\alpha=0{\cdot}2}} = 0{\cdot}93\varepsilon\frac{S_d^{0{\cdot}04}}{C_d^{0{\cdot}84}} \tag{24b}$$

## IMPLICATIONS FOR DESIGNING WITH VISCOUS DAMPERS

In its most general form equation (23) can be efficiently utilized in the preliminary as well as in the final design stages involved in designing a wide variety of viscous dampers for structures. The relationship given in equation (23) is in fact very suitable for the recommended design procedures recently introduced in FEMA 273/274.[4,5] These procedures employ the so-called Capacity Spectrum Method whereby the lateral (base shear) *capacity–displacement* curve of the structure (which is referred to as the 'pushover' capacity) is compared to the acceleration–displacement demand response spectrum.[1,2] The response of a structure is estimated graphically as the point where the pushover curve of the structure obtained via non-linear static analysis or simplified methods,[12] intersects the elastic demand as shown in Figure 10.

In the capacity spectrum method, the total effective damping is defined by the equivalent viscous damping at a given deformation on the capacity curve. Hence, the total effective damping represents all energy dissipation mechanisms of the structure and includes inherent viscous damping $\xi_0$; damping associated with inelastic action, $\xi_{hy}$; and supplemental damping, $\xi_d$, etc. In general, the effective (secant) period and the hysteric damping for a structure are amplitude-dependent. The effective period is the same as the initial period up to the yield response and the effective hysteretic damping is equal to the assumed inherent viscous damping (usually 5 per cent critical). After yield, the effective period lengthens and the effective damping typically increases as the inelastic deformations take place. However, in all cases, a unique value of total effective damping can be calculated for each spectral displacement on the capacity curve.

The damping due to structural yielding can be determined as (Figure 10)

$$\xi_{hy} = \frac{1}{4\pi}\frac{E_D}{E_S} \tag{25}$$

where

$$E_D = 4X_y X_{max}(K_0 - K_{eff}) \text{ and } E_S = K_{eff}X_{max}^2/2 \tag{26}$$

in which effective stiffness, $K_{eff}$ can be written in terms of ductility ratio $\mu$ as

$$K_{eff} = K_0(\alpha_s + (1 - \alpha_s)/\mu) \tag{27}$$

 

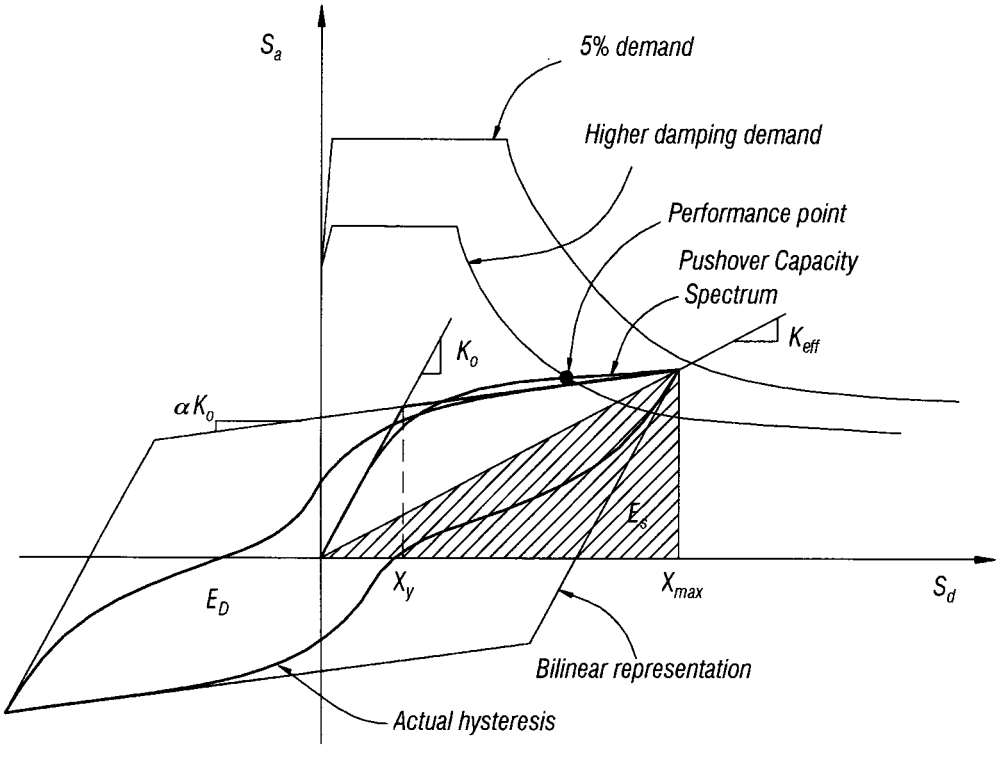


Figure 10. Capacity-demand spectrum

Therefore, assuming an overall bilinear pushover response as shown in Figure 10, effective damping due to hysteresis can be calculated by substituting equations (26) and (27) into equation (25) and rearranging to obtain

$$\xi_{\text{eff}} = \xi_0 + \xi_{\text{hy}} = \xi_0 + \frac{2}{\pi}\eta\frac{(1-\alpha_s)(1-1/\mu)}{(1-\alpha_s+\mu\alpha_s)} \tag{28}$$

where $\xi_0$ is the inherent damping, $\xi_{\text{hy}}$ the hysteric damping, $\mu = X_{\max}/X_y$ is the displacement ductility, $\alpha_s$ the post yield to initial stiffness ratio, and $\eta$ the efficiency factor defined as the ratio of the actual area enclosed by the hysteresis loop to that of the assumed perfect bilinear hysteresis (Figure 10). The efficiency factor is influenced by bond slip or pinching effect in reinforced concrete and by the Bauschinger effect in steel structures as well as the type of construction. Typical values range between 0·2 and 0·6 for concrete and steel structures, respectively.

In a similar manner, added damping due to supplemental viscous dampers can be taken into account using equation (23). Hence the total effective damping defined in equation (28) becomes

$$\xi_{\text{eff}} = \xi_0 + \xi_{\text{hy}} + \xi_d \tag{29}$$

 

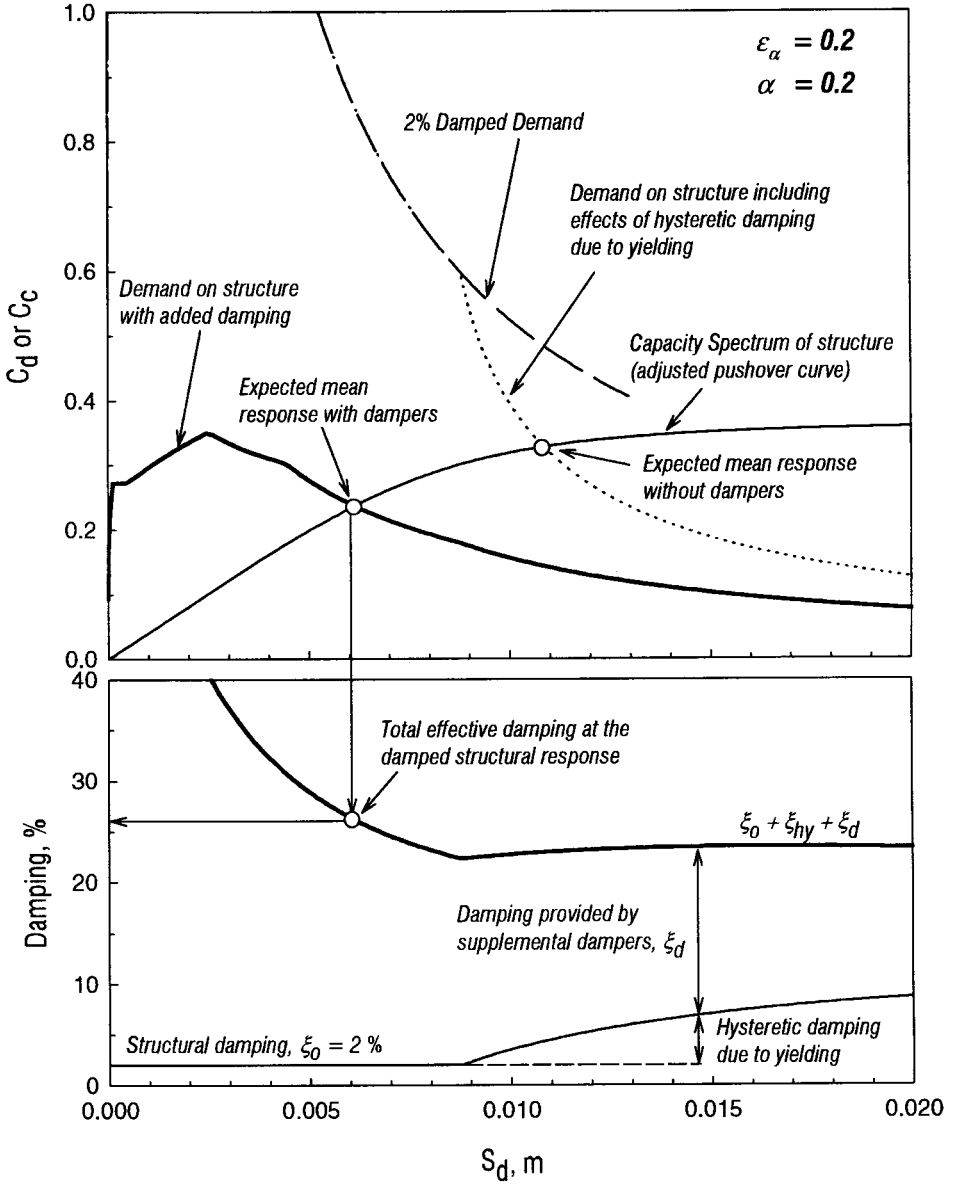


Figure 11. Graphical interpretation of design procedure

Application of the design procedure, described above, is depicted graphically in Figure 11. The corresponding *reduced* demand curves for undamped and for one particular damper capacity $\varepsilon_\alpha = 0{\cdot}2$ ($\alpha = 0{\cdot}2$) is plotted for the modified structure (due to added supplemental damping). In this figure, it is assumed that the stiffness properties of the structure (structural capacity) are not affected due to supplemental viscous devices. This procedure yields a single demand curve, which

 

intersects the capacity (adjusted pushover) curve at the performance point as shown in the figure. The required damper capacity can thus be determined (graphically if desired) depending on the specified performance objectives.

## CONCLUDING REMARKS

Many design codes are either in the process of developing or have recently incorporated methodologies that specifically address issues related to the design of supplemental energy dissipating devices such as non-linear viscous dampers. Hence, equivalent linear properties of these devices are utilized along the capacity-demand spectrum method. The equivalent linear properties are traditionally determined based on the equivalent energy consumption approach in which approximate-pseudo-spectral velocities are utilized. The approach used in present practice[4,5] has two inherent approximations: (i) the determination of equivalent viscous damping; and (ii) the implicit, but erroneous, assumption that the spectral velocity ($S_v = \omega_0 S_d$) is the same as the maximum structural velocity.

In this paper, the significance of these approximations was discussed and the differences illustrated. Due to the apparent velocity-dependent behaviour of the supplemental damping devices, it is recommended that the *actual* spectral velocities should be used in the design of such devices. For this purpose, 36 ground motions and their components were used to generate average pseudo and *actual* velocity spectra. Empirical expressions were obtained that enable transformations between pseudo and *actual* velocities as a function of damping, which were then simplified for use in design formulations.

Simplified velocity transformation rules were utilized in the proposed equivalent power consumption approach to determine the equivalent viscous properties of non-linear viscous dampers. It was shown that the equivalent power consumption formulation gives improved agreement to the exact solution compared to the equivalent energy formulation, particularly for the periods of interest for structures ranging from 0·5 to 3·0 sec. Moreover, the proposed equivalent power consumption approach provides a more direct and reliable relationship that can be easily incorporated in the preliminary as well as final design stages. This was demonstrated via the use of a normalized damper capacity term ($\varepsilon$) which is expressed as the maximum [non-linear] viscous damper force at a reference velocity as a percentage of the structural weight. The graphical design procedure, which is in fact an extension to the capacity-demand spectrum approach, may considerably facilitate the design of viscous devices.

### ACKNOWLEDGEMENTS

This study was undertaken in the Department of Civil, Structural and Environmental Engineering at the State University of New York at Buffalo. Financial support was primarily provided by a grant through Jarret, Inc. Funding was also provided under the "Year 11" program by the Multidisciplinary Center for Earthquake Engineering Research (MCEER, formerly NCEER) through a grant from the National Science Foundation (NSF). Both sources of support are gratefully acknowledged.

### REFERENCES

1. C. Kircher, 'Status Report of Structural Engineers Association of California (SEAOC) – Ad-Hoc Ground Motion committee,' *Presentations at SEAOC Annual Convention*, Sottsdale, 1993.

 

2. S. A. Freeman, 'The capacity spectrum method for determining the demand displacement', *Technical Session*: *Displacement Considerations in Design of Earthquake–Resisting Buildings*, ACI 1994 Springer Convention, 1994.
3. J. A. Mahaney, T. F. Paret, B. E. Kehoe and S. A. Freeman, 'The capacity spectrum method for evaluating structural response during the loma prieta earthquake', *Proc. 1993 Nat. Earthquake Conf*., 1993.
4. FEMA 273, 'NEHRP Guidelines for the Seismic Rehabilitation of Buildings', *Federal Emergency Management Agency*, 1997.
5. FEMA 274, 'NEHRP Commentary on the Guidelines for the Seismic Rehabilitation of Buildings', *Federal Emergency Management Agency*, 1997.
6. T. T. Soong and M. C. Constantinou, (eds), *Passive and Active Structural Vibration Control in Civil Engineering*, Springer, New York, 1994.
7. R. W. Clough and J. Penzien, *Dynamics of Structures*, 2nd edn., McGraw Hill, New York, 1993.
8. M. C. Constantinou, T. T. Soong and G. F. Dargush, (eds), *Passive Energy Dissipation Systems for Structural Design and Retrofit*, Monograph Series—1, Multidisciplinary Center for Earthquake Engineering Research, Buffalo, New York, 1998.
9. N. M. Newmark and W. J. Hall, *Earthquake Spectra and Design*, Earthquake Engineering Research Institute, Oakland, CA, 1982.
10. A. K. Chopra, *Dynamics of Structures*: *Theory and Applications to Earthquake Engineering*, 1st edn, Prentice-Hall, Englewood Cliffs, NJ, 1995.
11. G. Pekcan, J. B. Mander and S. S. Chen, 'The seismic response of a 1:3 scale R.C. structure with elastomeric spring dampers', *Earthquake Spectra* **11**(2), 249–267 (1995).
12. G. Pekcan, 'Design of seismic energy dissipation systems for reinforced concrete and steel structures', *Ph.D. Dissertation*, State University of New York at Buffalo, 1998.

 